CARBON CYCLING AND OCEAN MODELLING

The importance of the cycling of carbon and nitrogen as a major influence on global climate has been recognized for the past few decades, starting with the pioneering work of Keeling, Tans, Bryan, Manabe and others (IPCC 1992-2017). At CSIR-4PI, we have continued our intense research on modelling and simulation of the global carbon cycle as well as state-of-the-art measurements of greenhouse gases. These measurements are being assimilated into inverse transport models to yield robust fluxes of carbon. CSIR has funded a major project "Carbon Nitrogen Cycling in the Earth System (CNCES)" to enable us to continue our research in this important area.

Sensitivity of one of the parameters related to iron limitation $(Fe:N)_{irr}$ (which alters light utilization efficiency by phytoplankton) on primary productivity, chlorophyll, nitrate, pCO_2 and carbon flux in the Arabian Sea has been investigated. Numerical simulations of a marine biogeochemical model at a resolution of 0.25 degree is set up in the global domain for the estimation of marine productivity.

From the measurement side, we have been able to resume operations at our stations in Hanle and Pondicherry. The former has the potential of being a baseline station for monitoring the secular increase in GHG concentration. The station at Hoskote, which is also a primary reference calibration station has been operational and its stability has been demonstrated.

Inside

- Effect of iron limitation on the specific growth rate of phytoplankton
- Carbon cycle studies of the Indian Ocean using ocean biogeochemical model simulations and observations
- Greenhouse Gases (GHG) data collection and processing

1.1 Effect of iron limitation on the specific growth rate of phytoplankton

Sensitivity of one of the parameters related to iron limitation $(Fe:N)_{irr}$ (which alters light utilization efficiency by phytoplankton) on primary productivity, chlorophyll, nitrate, pCO_2 and carbon flux in the Arabian Sea has been investigated using a 3-D coupled Biogeochemical Model (TOPAZ) embedded in Modular Ocean Model (MOM4P1) in the global domain for climatology and interannual variability. Initially the model results are evaluated for many of the biogeochemical components using data from World Ocean Atlas, satellites and cruises in the Arabian Sea. It is noticed that model results capture seasonal and interannual variations of some of the biogeochemical components and fluxes in the Arabian Sea.
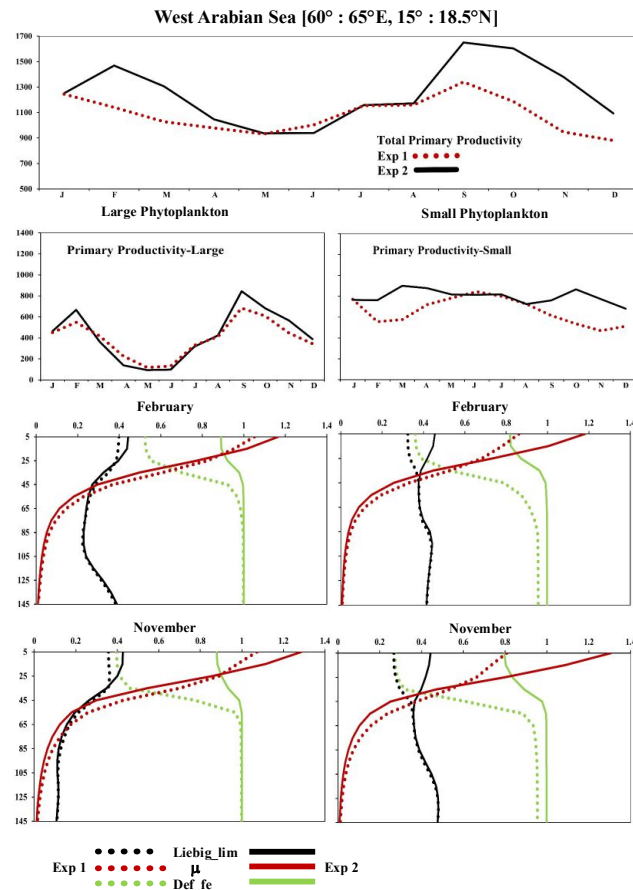

Figure 1.1 Comparison of Primary Productivity (mgC/m²/d) and Terms related to Specific Growth Rates of Large and Small Phytoplankton from model simulations Exp (1) and Exp (2) in the west Arabian Sea

To understand the effect of iron limitation parameter on the primary productivity, detailed analysis of the deficiency of Iron (through chlorosis factor which is a function of Fe:N ratio, which modulates Chl:N ratio), Leibig Limitation for nutrient uptake, Specific Growth rates for Large and Small Phytoplankton are carried out. It is noted that if $(Fe:N)_{irr}$ is decreased, Chlorosis is increased (i.e., iron limitation is reduced), specific growth rate for large and small phytoplankton are increased during some months and at some regions in the Arabian Sea which is reflected in the increase of primary productivity for both large and small phytoplankton. Figure 1.1 shows the terms which are responsible for determining the

Specific Growth Rate of Phytoplankton for two numerical simulations with different values of $(Fe:N)_{irr}$ namely, Exp(1) and Exp(2) for one region in the west Arabian Sea. It is clearly seen that when primary productivity is higher for Exp(2) compared to Exp(1) in west Arabian Sea, specific growth rate and chlorosis are higher for both large and small phytoplankton and also, the effect of iron parameter is higher for small phytoplankton compared to large phytoplankton. It is also noted that there is no change in primary productivity when $(Fe:N)_{irr}$ is decreased in the east of 65° E in the Arabian Sea. This study has shown that primary productivity and chlorophyll increase, nitrate and pCO_2 decrease during January-March and September-December, when iron limitation is reduced in the north and north-west regions of the Arabian Sea. But in the east Arabian Sea and regions of Arabian Sea south of 10º N, primary productivity, chlorophyll, nitrate, pCO_2 and carbon flux did not show any change when iron limitation is varied (figure not shown). Further analysis on the parameters and processes related to primary productivity of large and small phytoplankton need to be carried out to understand the limitations due to different micro and macro nutrients.

1.2 Carbon cycle studies of the Indian Ocean using ocean biogeochemical model simulations and observations

Simulations of global ocean biogeochemical model (TOPAZ) is used to study the influence of ocean physics on various biological and chemical processes in the north Indian Ocean. The model is integrated using different sets of forcing products to study the effect of thermal structure and ocean circulation on seasonal variations of productivity, nutrient transport and pCO_2 in the north Indian Ocean. Results of the simulations have been validated against available data (ARGO, MODIS, SeaWiFS, World Ocean Atlas etc.) on temperature, salinity, mixed layer depth, pCO_2, chlorophyll, primary productivity, nitrate and oxygen, for seasonal, interannual and annual variations to ascertain the model's capability to reproduce many of the significant features in the Arabian Sea (AS) and Bay of Bengal. Figure 1.2 shows the monthly variations of depth integrated chlorophyll, mixed layer depth, primary productivity and pCO_2 in the North Arabian Sea (Region:60°-66°E Longitude, 22.5°-24.5° N Latitude) for the period 1996 to 2009. It is observed that the mixed layer is deep in the north Arabian Sea, and influences the distribution of phytoplankton biomass and primary production. Also, the variations of depth integrated chlorophyll, primary productivity alters pCO_2 in this region.
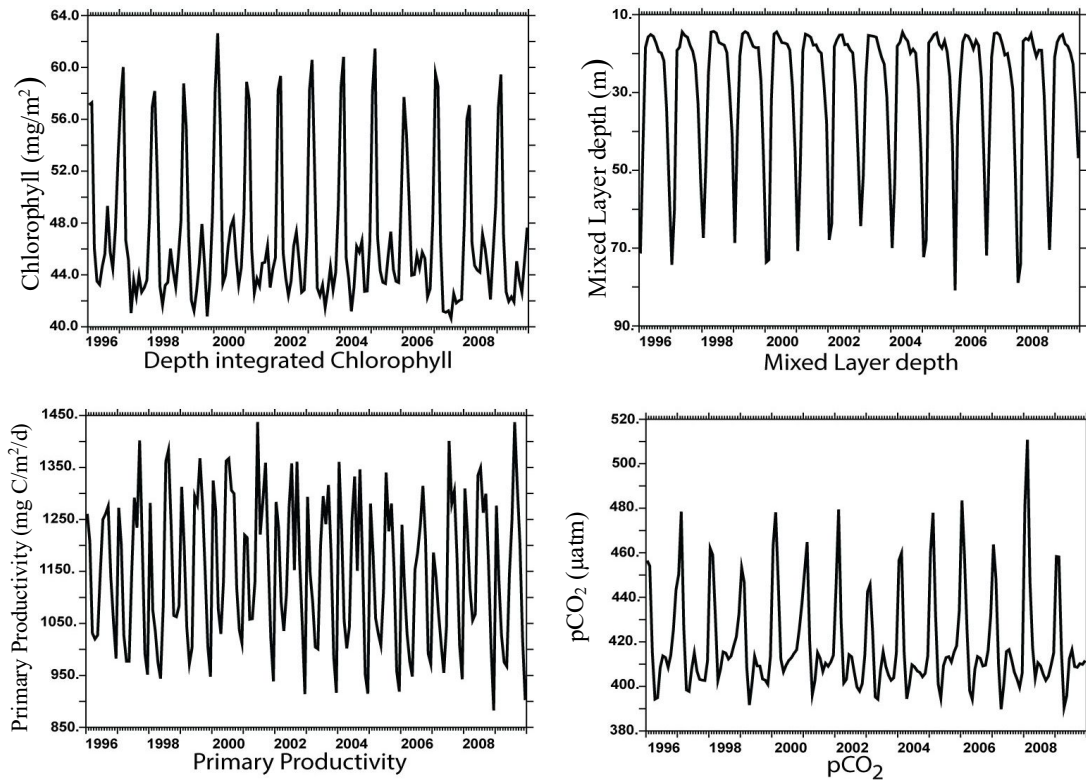
Region: 60°-66°E, 22.5°-24.5°N

Figure 1.2 Monthly variations of Depth Integrated Chlorophyll (mg/m^2), Mixed Layer Depth (m), Primary Productivity (mgC/m^2/d) and pCO$_2$ (μatm) in the North Arabian Sea (Region: 60°-66°E Longitude, 22.5°-24.5° N Latitude) during 1996 to 2009

## 1.3 Greenhouse Gases (GHG) Data Collection and Processing

Data collection at Hanle was resumed in Oct 2018 after the installation of the repaired Picarro G2301 instrument. The station is at a height of 4500 m and its elevation and surroundings (dry desert) are quite comparable to Mauna Loa, which is at a height of 3400m surrounded by volcanic lava with very little vegetation. The station is ideally suited to be a baseline station where the background GHG concentration can be monitored. We have applied the same technique that NOAA applies to process the data to extract the background signal. If two adjacent hourly averages differ more than 0.25 ppm, they are both discarded. Daily averages are computed for each month and a least squares spline is fit through this data. Outliers (2sigma) of hourly data from this curve are omitted and the process is iterated till no more data is excluded. Figure 1.3 shows the processing of CO$_2$ data for three months from October to December 2018.

The data points that survive this data selection are considered in the next step where a curve of a quadratic polynomial and two harmonics is fitted. Around 93% of the data survive after the data selection in Hanle after removal of local effects. The residuals from this fit are band pass filtered using FFT and its inverse is added to the least squares curve. This final

signal is taken to represent the baseline CO_2 values at Hanle. The processing of methane (CH_4) data is similar but the cut-offs are much smaller. Figure 1.4 shows daily averages of CO_2 and CH_4 data selected after the above procedure and the final curve fit.

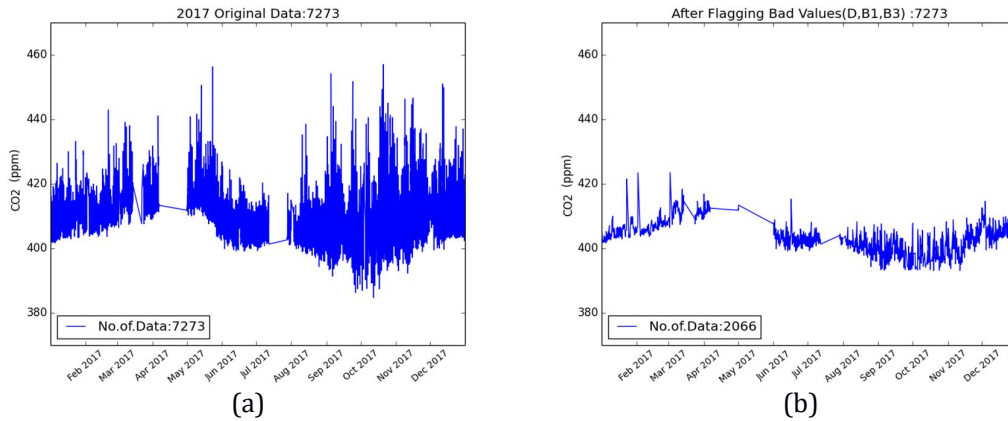(a)   (b)
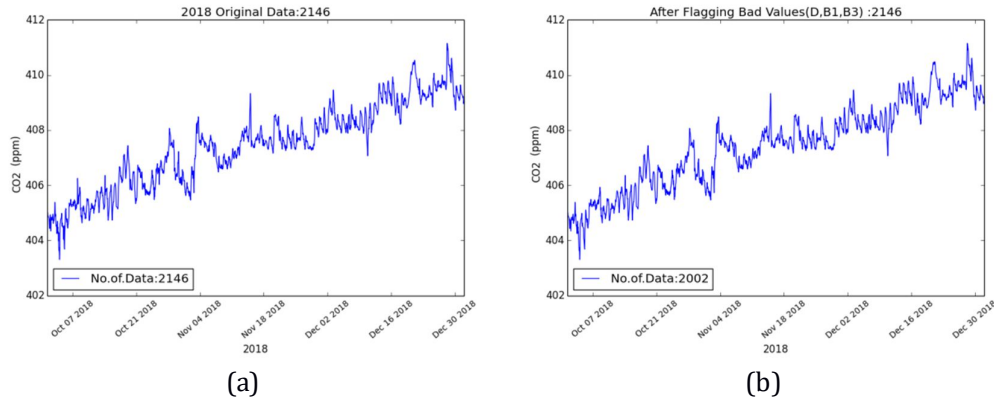
Figure 1.3 (a) Values before the data selection (b) Selected data after considering hour to hour difference and standard deviation cutoff for further processing

(a)   (b)

(c)   (d)
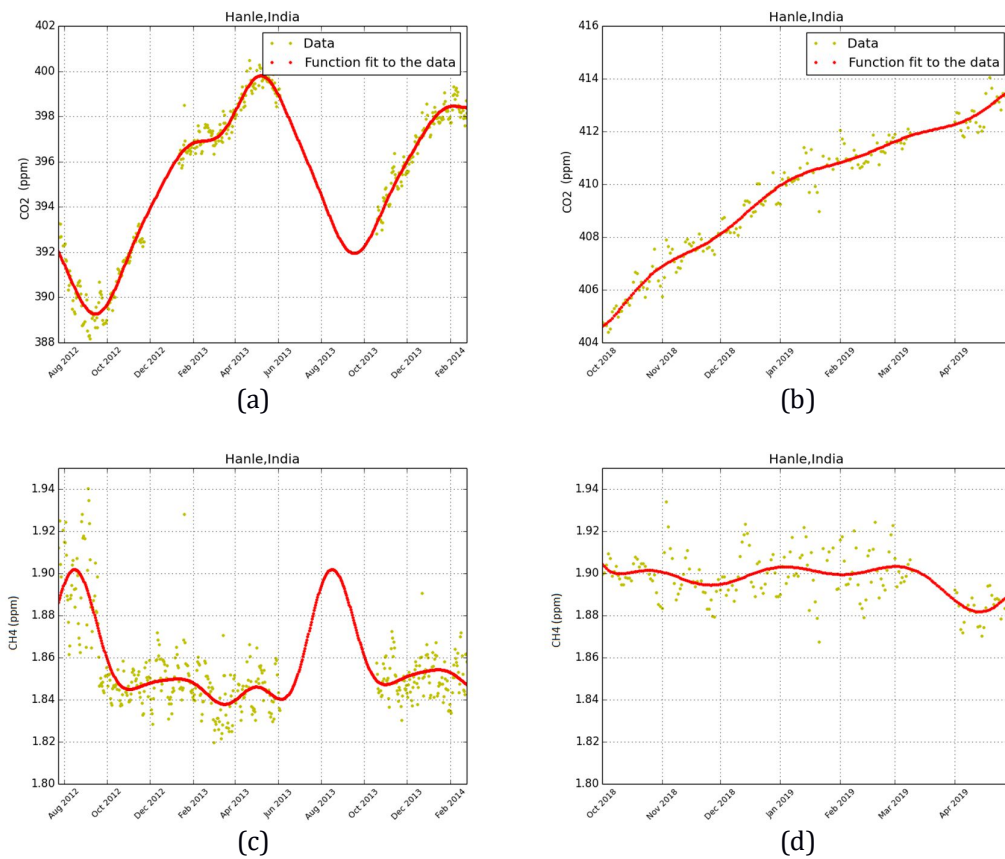
Figure 1.4 (a) Past data fit of CO_2 for 2012-2014 (b) CO_2 data fit from October 2018 onwards (c) CH_4 data fit for 2012-2014 (d) CH_4 data fit from October 2018 onwards

The GHG station at Hoskote has been operating since Nov. 2016 and we have a continuous record for nearly the whole period. However, the station is not isolated from local influences as Hanle. The extraction of background signals at Hoskote is much more complicated as we

try to exclude the effects of local sources and sinks. Figure 1.5 shows processing of CO_2 data in Hoskote for 2017 as a representative.

(a)   (b)

Figure 1.5 (a) Data before the selection   (b) Data selected after considering hour to hour difference and standard deviation cutoff for further processing.

Further the CO_2 data processed in Hoskote is represented in Figure 1.6 to show different criteria for flagging values viz. Night time data, hourly variability, standard deviation cutoff, outliers. After applying the selection process described earlier, less than 20 percent of the data survive for further processing.
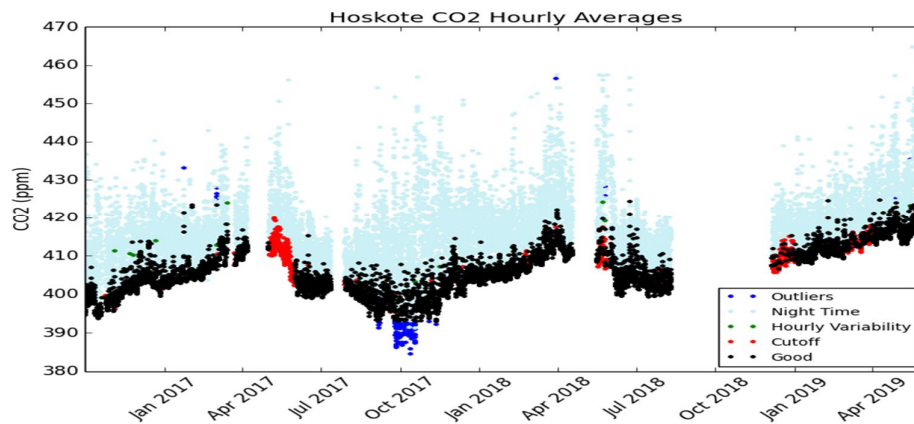
Figure 1.6 Representation of CO_2 data in different categories

In Hoskote, Methane (CH_4) is also measured by the same instrument whereas Carbon monoxide (CO) and Nitrous oxide (N_2O) are measured by another instrument LGR. A similar procedure for data selection and curve fit is applied to these data as well. Figure 1.7 shows the daily averages of the selected data of CO_2, CH_4, CO and N_2O and the final curve fit obtained by the procedure as explained earlier for the processed data for 2016-19.
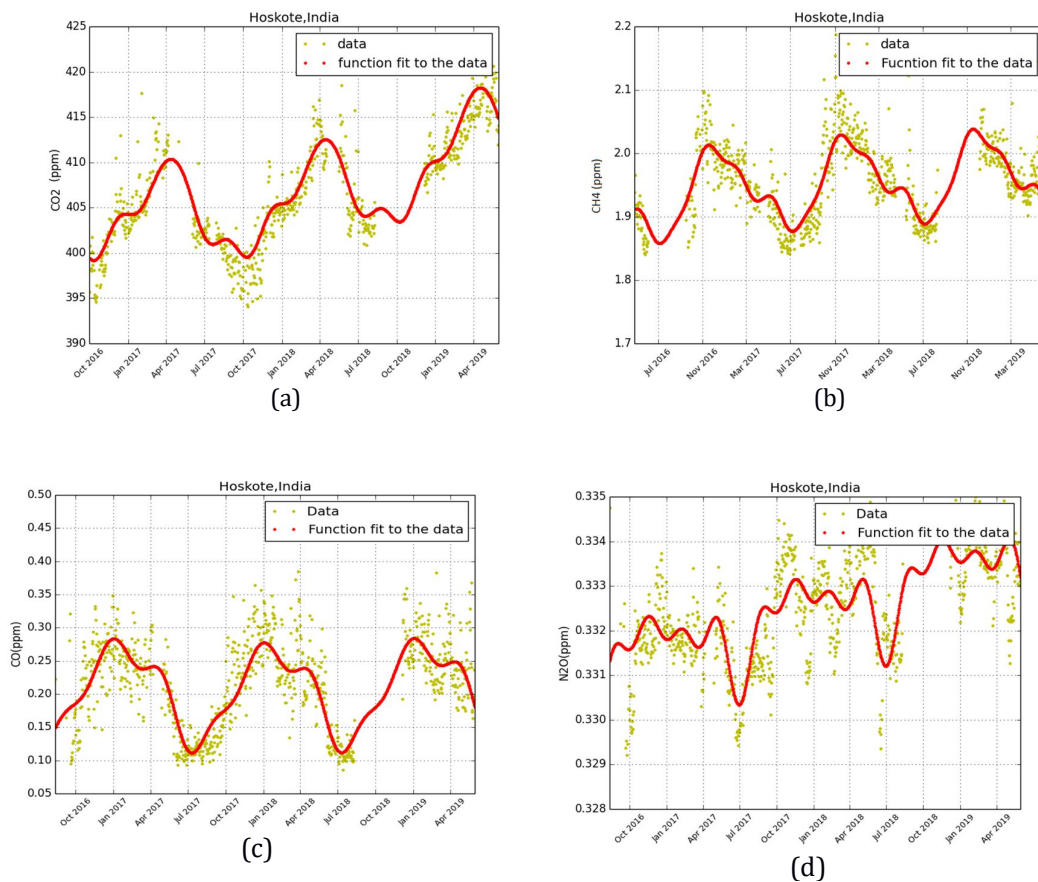
Figure 1.7 (a) CO_2 data is represented with the function fit (b) CH_4 data is represented with the function fit (c) CO data is represented with the function fit (d) N_2O data is represented with the function fit

Data collection at Pondicherry was resumed in March 2019 after the Picarro instrument was replaced with a new repaired one. The CO_2 and CH_4 data are under process.

The GHG station at Hoskote is also equipped with primary cylinders supplied from NOAA. The two instruments measuring these GHGs are calibrated with a set of secondary cylinders which are called working standards. These secondary cylinders are calibrated with the NOAA primary cylinders once a year.

Table 1.1 gives the comparison between the calibrated values for all the six secondary cylinders in 2017 and 2018 for each of the four species that are measured. It is seen that the cylinders are very stable as there has been very little drift in the values between the two years.

Using the short target values measured by the instrument after every measurement cycle of the ambient air, it is interesting to see that the measurement is very stable and the instrument has not drifted.

Table 1.1 Comparison of the calibrated values of secondary cylinders done in 2017 and 2018

Species : CO2 (ppm)

TANK	CYLINDER	Calibrated value 2017	Calibrated Value 2018
		CO2 (ppm)	CO2 (ppm)
CAL 1	D300571	372.11175198	372.101360041
CAL 2	D300560	402.345977102	402.33697978
CAL 3	D300567	423.088349966	423.091939458
CAL 4	D300559	483.357980321	483.366888558
TGT_LG	D300572	461.189882606	461.197281736
TGT_ST	D300562	402.404705726	402.418704366

Species : CH4 (ppb)

TANK	CYLINDER	Calibrated value 2017	Calibrated Value 2018
		CH4 (ppb)	CH4 (ppb)
CAL 1	D300571	1831.46671208	1831.77964386
CAL 2	D300560	1926.54621005	1926.74516346
CAL 3	D300567	2127.15906146	2127.32374738
CAL 4	D300559	2424.27975298	2424.62790278
TGT_LG	D300572	2322.28630188	2322.10150743
TGT_ST	D300562	1926.75812441	1926.92472519

Species : CO (ppb)

TANK	CYLINDER	Calibrated value 2017	Calibrated Value 2018
		CO (ppb)	CO (ppb)
CAL 1	D300571	52.653245716	53.5441083586
CAL 2	D300560	100.529999052	101.11639529
CAL 3	D300567	250.977132704	251.193593545
CAL 4	D300559	496.340578348	494.997452872
TGT_LG	D300572	496.713380831	494.89882726
TGT_ST	D300562	153.615536353	154.748998853

Species : N2O (ppb)

TANK	CYLINDER	Calibrated value 2017	Calibrated Value 2018
		N2O (ppb)	N2O (ppb)
CAL 1	D300571	318.179357735	318.328337649
CAL 2	D300560	337.761495567	337.173362327
CAL 3	D300567	342.93842041	342.346346422
CAL 4	D300559	358.68563159	358.292213299
TGT_LG	D300572	349.373881061	348.789229332
TGT_ST	D300562	336.528950158	336.061861005

Figure 1.8 shows the instrument measuring CO_2 for the short target cylinder, having 402.4 ppm of concentration of CO_2, over three months is very stable. The same is true for all the other three species and hence both the instruments are very stable.

(a)   (b)
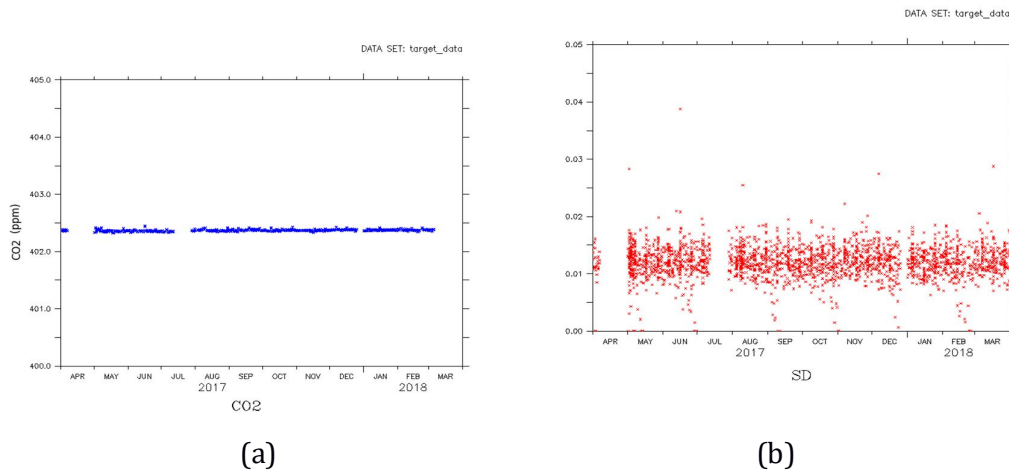
Figure. 1.8 (a) Short Target of CO_2 in Hoskote (b) Standard deviation of minute means of CO_2 for short target